Adsorption Free Energy of Phenol Onto Coronene: Solvent and Temperature effects

Alhadji Malloum[†,◇,*] and Jeanet Conradie[†,‡]

[†] Department of Chemistry, University of the Free State, PO BOX 339, Bloemfontein 9300, South Africa.

[◇] Department of Physics, Faculty of Science, University of Maroua, PO BOX 46, Maroua, Cameroon.

[‡]Department of Chemistry, UiT - The Arctic University of Norway, N-9037 Tromsø, Norway.

November 5, 2022

ABSTRACT: Molecular modeling can considerably speed up the discovery of materials with high adsorption capacity for wastewater treatment. Despite considerable efforts in computational studies, the molecular modeling of adsorption processes has several limitations in reproducing experimental conditions. Handling the environmental effects (solvent effects) and the temperature effects are part of the important limitations in the literature. In this work, we address these two limitations using the adsorption of phenol onto coronene as case study. In the proposed model, for the solvent effects, we used a hybrid solvation model, with n explicit water molecules and implicit solvation. We increasingly used $n = 1$ to $n = 12$ explicit water molecules. To account for the temperature effects, we evaluated the adsorption efficiency using the adsorption free energy for temperatures varying from 200 to 400 K. We generated initial configurations using classical molecular dynamics, before further optimisation at the ωB97XD/aug-cc-pVDZ level of theory. Polarizable continuum solvation model (PCM) is used for the implicit solvation. The adsorption free energy is evaluated to be -1.3 kcal/mol at room temperature. It has been found that the adsorption free energy is more negative at low temperatures. Above 360 K, the adsorption free energy is found to be positive.

KEYWORDS: Adsorption, Adsorption free energy, Solvation, Temperature effects

1 Introduction

Research on wastewater treatment has received considerable attention from both computational researchers and experimentalists. A *Scopus* (www.scopus.com) search using the keyword "wastewater treatment" generates approximately 164132 documents which highlights the volume of work in this research field. Adsorption is one technique used in wastewater treatment. The aim of adsorption is to identify cheap and abundant materials to adsorb pollutants. Up to now, most of the works performed on the adsorption of pollutants are based on experimental investigations, which is desirable. However, experimental investigations are slow and require considerable resources (both human and financial). On the other hand, computational studies can save both time and resources in identifying materials with high adsorption capacity. Thus, a cheaper route in identifying suitable materials is to use computational studies to identify potential materials with high adsorption capacity, for further experimental investigation. In prelude to experimental investigation, in this view, computational studies are performed to screen over a large number materials to identify the most important ones. This will then save both experimental time and resources. The main challenge in computational studies is the realistic modeling of pollutant and the adsorbent during the adsorption process. To be reliable, a molecular modeling of adsorption processes has to be as close as possible to the experimental conditions. Up to now, this remains the important challenge of molecular modeling of adsorption processes.

Adsorption of phenol onto activated carbon has been reported by Cam, Khu and Ha [1] using density functional theory (DFT). Implicit solvation has been account for using the COSMO solvation model. The activated carbon is represented by a bended surface of graphene. The adsorption energy has been evaluated using the electronic energy. The maximum adsorption energy is calculated to be -25.8 kcal/mol [1]. Húmpola *et al.* [2] have reported the investigation of the adsorption of phenolic compounds onto different models of graphene. The investigations were performed using DFT, semi-empirical quantum mechanics, and Monte-Carlo simulations. The authors concluded that based on their investigations there is no evidence of $\pi\cdots\pi$ interactions during the adsorption of phenolic compounds onto graphene. Adsorption of ethyl mercaptan onto some models of activated carbon has been also investigated [3]. The authors used B3LYP/6-31++G(d,p) level of theory, and calculated the adsorption energy using the electronic energy [3]. Furthermore, different models of activated carbons have been used for the extraction of ibuprofen from wastewater [4]. The investigations have been performed using grand canonical Monte Carlo simulations. Zhou *et al.* [5] have reported the adsorption of volatile organic compounds onto some models of activated carbon using DFT. The authors have not considered the solvation effects, and the adsorption energy is calculated using the electronic energy [5]. Recently, adsorption of benzene onto different models of activated carbon is reported by Li *et al.* [6]. Four models of activated carbon have been studied using grand canonical Monte Carlo simulations [6]. Liu *et al.* [7] investigated the adsorption of phenol onto some pristine graphene molecules (also called activated carbon) using DFT. The investigations have been performed at the PW91/DNP level of theory. Different models of activated car-

* *E-mail: MalloumA@ufs.ac.za; Tel: +237 695 15 10 56*

bons have been assessed: pristine, amine pristine, pyridine pristine, and pyrrole pristine. The authors used the COSMO implicit solvation model, to account for the environmental effects. The adsorption energy is calculated using the electronic energy at 0 K. The authors found that amine pristine has the highest parallel adsorption energy (-13.4 kcal/mol), while pyridine pristine has the highest side adsorption energy (-13.6 kcal/mol)[7].

The literature mining shows that computational modeling of adsorption has two main limitations: handling of temperature and solvent effects. As noted in previous works, almost all the authors have calculated the adsorption energy using the electronic energy, which does not consider the temperature. Regarding the solvent effects, either they are not considered or they are considered through implicit solvation. Very recently, we assessed four solvation schemes to study the adsorption of aniline onto coronene[8]. The first scheme comprises the aniline and coronene in gas phase, while the second scheme comprises the aniline and coronene in implicit water solvent. The third scheme is constituted of aniline + coronene + six explicit water molecules, while the fourth scheme is constituted of aniline + coronene + six explicit water molecules all in implicit water solvent[8]. The results show that the adsorption free energy calculated within the four schemes are completely different, highlighting the importance of the choice of the solvation scheme. Obviously, the fourth scheme is the most reliable scheme due to its proximity with reality. In the fourth scheme, the water molecules that are around the system (aniline + coronene) are treated explicitly using quantum mechanics while the remaining water molecules (that are "far" from the system) are considered as a dielectric medium. Thus, the fourth scheme is both reliable and robust. However, in our previous work, we randomly chose six water molecules for the explicit solvation[8]. As stated in that work, the number of explicit water molecules can influence the adsorption free energy. Therefore, we undertook to investigate the effect of explicit water molecules for different temperatures. For this investigation, we use phenol as pollutant while coronene is used as adsorbent.

Phenol is an organic aromatic compound used in industries for different synthesis. The excess phenol not used in the synthesis is discharged in the environmental as a pollutant for water. Similar to pharmaceutical drugs, phenol is one of the recalcitrant pollutants. For the current case study of the solvent and temperature effects on the adsorption of pollutants, we used phenol as an example of pollutant. In addition, phenol is a relatively small molecule, allowing easy computational tractability as compared to some dye molecules, for example. On the other hand, activated carbon derived from different organic material constitute the most used adsorbent. Therefore, we used coronene (a model of graphene) as adsorbent. This choice is also motivated by the computational tractability of the generated systems (phenol + coronene + water molecules).

2 Methodology

We start this section by presenting the model used to describe the adsorption free energy (see subsection 2.1). Then, we explain how we performed the sampling of initial configurations of complexes Coronene-PhOH$(H_2O)_n$ and PhOH$(H_2O)_n$, $n = 1-12$ (see subsection 2.2). Finally, we present the computational details used in this work (see subsection 2.3).

2.1 Calculation of adsorption free energy

To take into account the effect of temperature, the adsorption power of adsorption efficiency is calculated using the Gibbs free energy instead of the electronic energy used in the majority of the works. Throughout the manuscript, we will refer to Gibbs free energy as free energy. In this work, to model the adsorption process, we consider coronene as adsorbent and phenol as pollutant. Thus, the adsorption free energy is calculated using Equation 1.

$$\Delta G^n_{Ads}(T) = G^n(T) - G_{PhOH(H_2O)_n}(T) - G_{Coronene}(T). \quad (1)$$

Where

$$G^n(T) = \sum_k W^n_k(T) \times G^n_k(T), \quad (2)$$

and

$$W^n_k(T) = \frac{\exp(-\beta G^n_k(T))}{\sum_i \exp(-\beta G^n_i(T))}. \quad (3)$$

$G^n_k(T)$ is the free energy of the $k-th$ isomer of Coronene-PhOH$(H_2O)_n$ at a given temperature T. $\beta = 1/K_BT$ is the Boltzmann constant. $W^n_k(T)$ is the weight of the $k-th$ isomer of Coronene-PhOH$(H_2O)_n$ at T. The free energy $G_{PhOH(H_2O)_n}(T)$ is also calculated the same way as $G^n(T)$, where Coronene-PhOH$(H_2O)_n$ are replaced by PhOH$(H_2O)_n$. Thus, both $G^n(T)$ and $G_{PhOH(H_2O)_n}(T)$ are calculated using Boltzmann weighted average. $G_{Coronene}(T)$ is the free energy of coronene at temperature T. As only one configuration of coronene is available, the free energy of coronene is not a Boltzmann average. A schematic representation of the model used to compute the free energy is reported in Figure 1. $W^n_k(T)$ as well as $G^n_k(T)$ are calculated using the program TEMPO[9,10].

As both coronene and phenol are in water, to model the environment of the system, we consider both explicit and implicit solvation. The schematic representation of Figure 1 shows the example with four explicit water molecules. For the explicit solvation, we successively use $n = 1$ to 12 explicit water molecules. Thus, the full system is constituted of coronene interacting with phenol and n explicit water molecules, all in implicit water solvent, Coronene-PhOH$(H_2O)_n$. The adsorption free energy is the binding energy between the coronene in implicit water and PhOH$(H_2O)_n$ in implicit water. As can be seen later (in Figure 3 to Figure 7), the explicit water molecules preferably bind to phenol. Thus, phenol and the n water molecules are considered to form a single block in the present model. This is also in line with reality, as phenol is already solvated by water molecules before even we start the adsorption process.

2.2 Sampling of configurations

As implicitly indicated in Equation 3, there are several possible configurations of the complex Coronene-PhOH$(H_2O)_n$ and

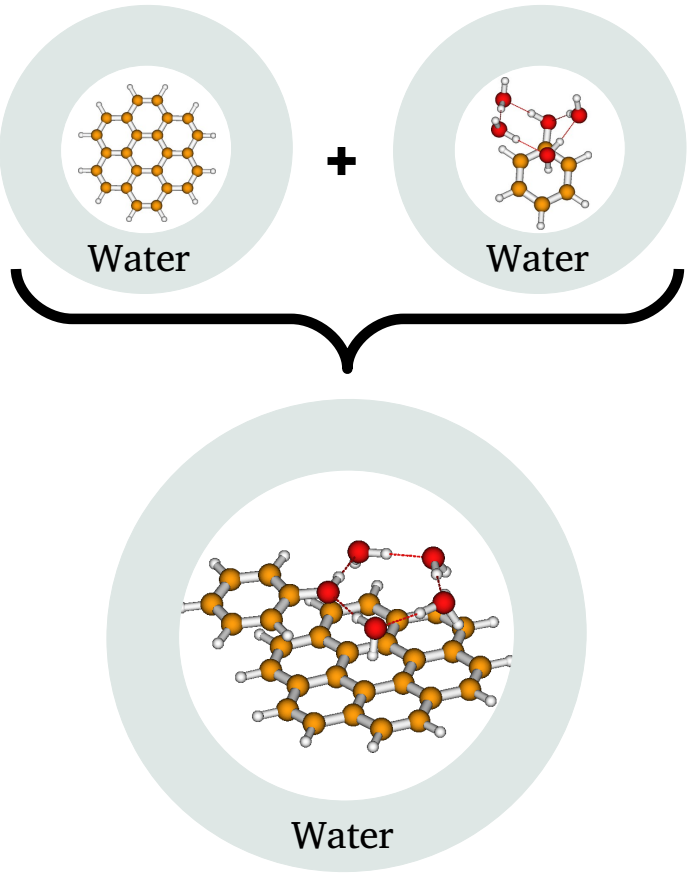

Fig. 1 Schematic representation of the model use in this work to compute the adsorption free energy of phenol onto coronene. The example is provided for the case of $n = 4$ explicit water molecule. The red surface represents the implicit dielectric continuum medium.

$PhOH(H_2O)_n$ for each given cluster size n. For accurate investigation, we need to generate all possible configurations of the aforementioned systems. To sample all the possible configurations, we used the ABCluster code of Zhang and Dolg [11,12]. ABCluster samples all possible configurations and classifies them from the most stable to the least stable configuration based on a classical energy. The classical energy used by ABCluster is constituted of Lennard-Jones potential as well as electrostatic potential. The parameters used are based on CHARMM's force field [13]. Details on how the configurations are generated can be found in our recent works [14–18]. In addition, the reader is advised to read the original papers of Zhang and Dolg [11,12] for more details on ABCluster.

2.3 Computational details

After sampling initial configurations using ABCluster, the configurations have been optimised using Gaussian 16 suite of programs [19]. All optimisation are performed using the ωB97XD [20] functional of DFT associated to the aug-cc-pVDZ basis set [21]. It is worth mentioning that the functional ωB97XD has been used in our previous works to calculate the binding energies of molecular clusters [22–25]. In those works, ωB97XD has shown good performance when benchmarked to DLPNO-CCSD(T)/CBS level of theory [26,27]. For accurate optimisation, we used the *tight* option. For integrals, *ultrafine* grid has been used for accuracy. Frequencies calculations are performed at the same level of theory. The frequencies are calculated to confirm the stability of the located structures (checking the non existence of imaginary frequencies), and to compute thermodynamics properties (especially the Gibbs free energies). Implicit solvation has been taken into account using the integral equation formalism polarizable continuum model (IEF-PCM).

3 Results and discussions

In this section, we first present the structures of the phenol-water clusters, $PhOH(H_2O)_n$ (see subsection 3.1). Then, we present the located structures of the complex Coronene-$PhOH(H_2O)_n$, for difference values of $n = 1 - 12$ (see subsection 3.2). With the structures of $PhOH(H_2O)_n$ and Coronene-$PhOH(H_2O)_n$ in hand, we finally calculated the adsorption free energy for $n = 1 - 12$ and for temperatures ranging from 200 to 400 K (see subsection 3.3).

3.1 Structures of $PhOH(H_2O)_n$

After thorough exploration of the potential energy surfaces (PESs) of $PhOH(H_2O)_n$ using ABCluster, the located structures are optimised at the ωB97XD/aug-cc-pVDZ level of theory. Only

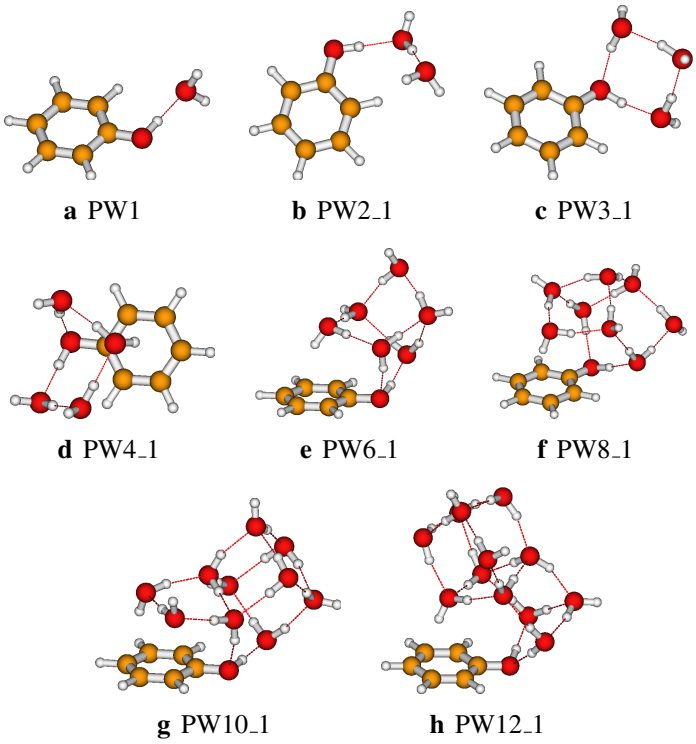

Fig. 2 Located most stable structures of $PhOH(H_2O)_n$, $n = 1 - 12$, as optimised at the ωB97XD/aug-cc-pVDZ level of theory. The structures are optimised in implicit water solvent using the PCM solvation model.

the most stable structures are reported in Figure 2. Although we reported only the most stable structures, for each cluster size, we used the Boltzmann average free energy and not just the free energy of the most stable structure. It is worth noting that the structures of the phenol-water clusters (up to the octamer) have been reported previously by some authors[28–33]. No global optimisation have been performed by the authors leading to local minima which are not global minimum energy structures. Apart from the phenol-water monomer and trimer, our reported most stable structures are different from the ones reported in previous works. This difference is most probably due to the fact that thorough exploration of PESs has not been performed in previous works. In addition, the structures are optimised in this work in the solvent phase, which could be another reason for the difference in the located structures.

Examination of the structures shows that the most stable structures establish strong OH···O, weak CH···O hydrogen bondings, and weak OH···π bonding interaction. We noted that the OH group of phenol in PhOH$(H_2O)_n$ participates in the hydrogen bond network the same way as the other explicit water molecules. The results show that the structures of phenol-water clusters have the same configuration as those of neutral water clusters[34–36]. However, in phenol-water clusters, the structures are folded due to the interactions of the water molecules of the phenyl group of phenol.

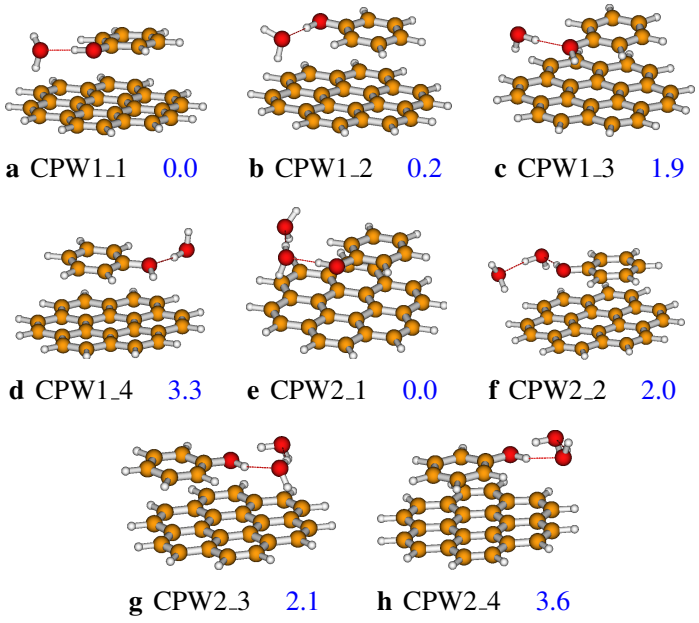

Fig. 3 Structures of Coronene-PhOH$(H_2O)_n$, $n = 1,2$, as optimised at the ωB97XD/aug-cc-pVDZ level of theory. The structures are optimised in implicit water solvent using the PCM solvation model. Numbers represent the relative electronic energies of the structures (in kcal/mol), and calculated at the ωB97XD/aug-cc-pVDZ level of theory.

3.2 Structures of Coronene-PhOH$(H_2O)_n$

Before calculating the adsorption free energies, one needs the structures of Coronene-PhOH$(H_2O)_n$ (CPW$_n$) for different values of n. We studied the structures of Coronene-PhOH$(H_2O)_n$ (CPW$_n$) for $n = 1$ to $n = 12$. The optimised structures of the complex for $n = 1$ and $n = 2$ are reported in Figure 3. For both CPW$_1$ and CPW$_2$, four possible configurations are located on their potential energy surfaces (PESs). In **CPW1_1**, the water molecule acts as proton acceptor. In **CPW2_1**, there are two strong OH···O hydrogen bondings, and one CH···O hydrogen bonding. It can be seen in Figure 3 that the most stable structures of CPW$_1$ and CPW$_2$ (**CPW1_1** and **CPW2_1**) correspond to the most stable structure of phenol-water monomer and dimer (**PW1** and **PW2_1** in Figure 2), respectively. Except for the coronene surface, the configurations of the two systems are found to be identical. For the CPW$_1$, the configurations where the water molecule acts as a proton donor are found to be the least stable configurations (see **CPW1_3** and **CPW1_4** in Figure 3). For the CPW$_2$, the least stable configuration located in this work has a cyclic configuration, and lies 3.6 kcal/mol above the most stable structure.

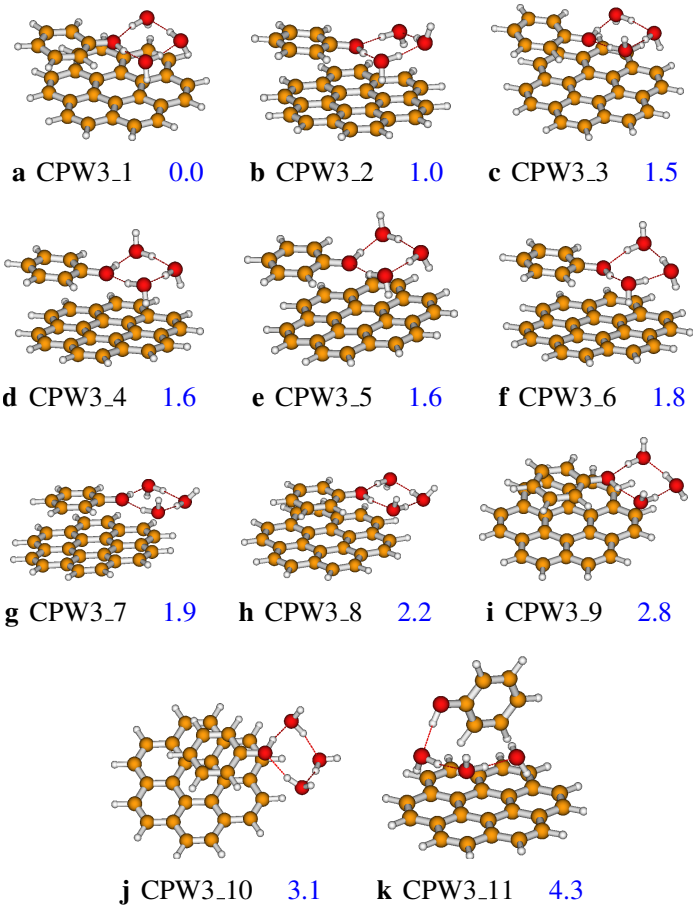

Fig. 4 Structures of Coronene-PhOH$(H_2O)_3$ as optimised at the ωB97XD/aug-cc-pVDZ level of theory. The structures are optimised in implicit water solvent using the PCM solvation model. Numbers represent the relative electronic energies of the structures (in kcal/mol), and calculated at the ωB97XD/aug-cc-pVDZ level of theory.

As far as the CPW_3 structures are concerned, eleven stable configurations have been located on its PES at the ωB97XD/aug-cc-pVDZ level of theory (reported in Figure 4). In addition, we found that the relative energies of the located structures span within 4.3 kcal/mol. Examination of the configurations shows that the most stable configurations have the phenyl group parallel to coronene, while less stable structures have their phenyl group perpendicular or non parallel to coronene. Furthermore, the most stable structure of CPW_3, **CPW3_1**, has cyclic configuration of the phenol-OH and the water molecules. **CPW3_1** is stabilised by four strong OH$\cdots$O hydrogen bondings, and three OH$\cdots\pi$ bonding interactions (see Figure 4). The difference between the cyclic configurations in **CPW3_1**-**CPW3_10** comes from the number of OH$\cdots\pi$ bonding interactions.

Thirty, twenty-six, and twenty-eight structures are located on the PESs of CPW_4, CPW_6, and CPW_8, respectively. The located configurations are reported in Figure 5, Figure 6, and Figure 7, respectively. In these figures, only the first twelve most stable configurations are reported. The complete lists of the located configurations of CPW_4, CPW_6, and CPW_8 are provided in the supporting information attached to the manuscript. Relative energies (in kcal/mol) are also reported in the figures (both in the manuscript and the supporting information). The results show that the most stable structure of CPW_4 has a cyclic configuration constituted of the explicit water molecules (see Figure 5). The corresponding phenol-water tetramer has a folded cyclic configuration (see Figure 2). As can be seen in Figure 5, the first 08 most stable structures have cyclic configuration of the phenol-OH and the water molecules. This is due to fact that cyclic configurations have strong OH$\cdots$O hydrogen bondings. The less stable configurations have less strong hydrogen bondings and smaller recovery between the phenyl group and the coronene molecule. The stability of the isomers is strongly affected by the recovery/overlap between the phenyl group and coronene. The higher the recovery, the higher the stability of the corresponding configuration. The recovery between the phenyl group and coronene expresses the number of possible $\pi\cdots\pi$ interactions. This observation applies also to the structures of CPW_6 and CPW_8. It can be seen the supporting information that the less stable structures of CPW_4, CPW_6, and CPW_8 have their phenyl group non-parallel to coronene reducing the recovery, and thus reducing the number of $\pi\cdots\pi$ interactions. As far as CPW_6 and CPW_8 are concerned, their most stable structures have cage-like configurations in agreement with phenol-water clusters and neutral water clusters[37–41]. It has been noted that the hydrogen bond networks in CPW_n is almost the same as the hydrogen bond networks of neutral water clusters[42–47].

For the Coronene-PhOH$(H_2O)_n$, $n = 10$ and $n = 12$, only the most stable geometries generated by ABCluster have been optimised at the ωB97XD/aug-cc-pVDZ level of theory. The optimised most stable structures are reported in Figure 8. The located structures have cage-like configurations same as the corresponding phenol-water clusters, and neutral water clusters[37,40,44,48]. It has been found that the located structure of CPW_{10} has its phenyl group parallel to coronene, enhancing therefore its stability. However, the phenyl group in CPW_{12} is non-parallel to coronene. A possible reason for the non-parallel is that the increase of the number of explicit water molecules requires considerable space, and do not permit phenyl to be parallel to coronene. It should be noted that none of the first 20 most stable configurations generated by ABCluster were parallel, whereas ABCluster generally gives good indication for stability order.

3.3 Adsorption free energy of phenol onto coronene

With the structures of Coronene-PhOH$(H_2O)_n$ and PhOH$(H_2O)_n$ in hand, we calculated the adsorption free energy and the adsorption enthalpy for temperature varying from 200 to 400 K. We plotted in Figure 9 the estimated adsorption free energy and enthalpy as function of the number of explicit water molecules n, at room temperature.

It comes out from Figure 9 that the adsorption free energy as well as the adsorption enthalpy at room temperature are slowly varying with increasing value of n. This could indicate that the estimated adsorption free energy and enthalpy, within the present model, are independent from the number of explicit water molecules. This remark is specific to the current system, and it is understandable. In the current system (coronene + phenol), only the OH group of phenol has close interaction with explicit water molecules. The OH group can only establish one or two strong hydrogen bondings with two water molecules. Therefore, above $n = 2$, the water molecules are not interacting with the system, and could be discarded. In conclusion, the number of explicit water necessary in this model is the number of water molecules enough to solvate the hydrophilic region of the system. In the present work, one or two explicit water molecules are enough. Averaging over the estimates, the adsorption free energy and the adsorption enthalpy are evaluated at room temperature to be -1.3 kcal/mol and -14.3 kcal/mol, respectively.

To assess the effects of temperature of the calculated adsorption free energy and adsorption enthalpy, we calculated these energies for temperatures varying from 200 to 400 K. We reported in Figure 10 the adsorption free energy and the adsorption enthalpy as function of temperature. The data used to plot Figure 10 as well as Figure 9 is provided in the supporting information. As can be seen in Figure 10, the adsorption free energy is linearly increasing with the increase of temperature. For all the values of n, the adsorption free energy is positive above 360 K, highlighting that the adsorption is not possible above this temperature. Thus, the increase of temperature does not favour the adsorption process, as the adsorption free energy is more negative at low temperatures. As far as the adsorption enthalpy is concerned, we have noted that the estimated values have negligible change with the change of temperature (see Figure 10). Thus, the adsorption enthalpy could be considered as temperature independent. The linear variation of the adsorption free energy, and the constant value of the adsorption enthalpy, indicate that the adsorption entropy is constant. The slope of the curves depend only on the adsorption entropy. Therefore, we conclude that the adsorption free energy is entropically driven.

One may think that the small value of the adsorption free en-

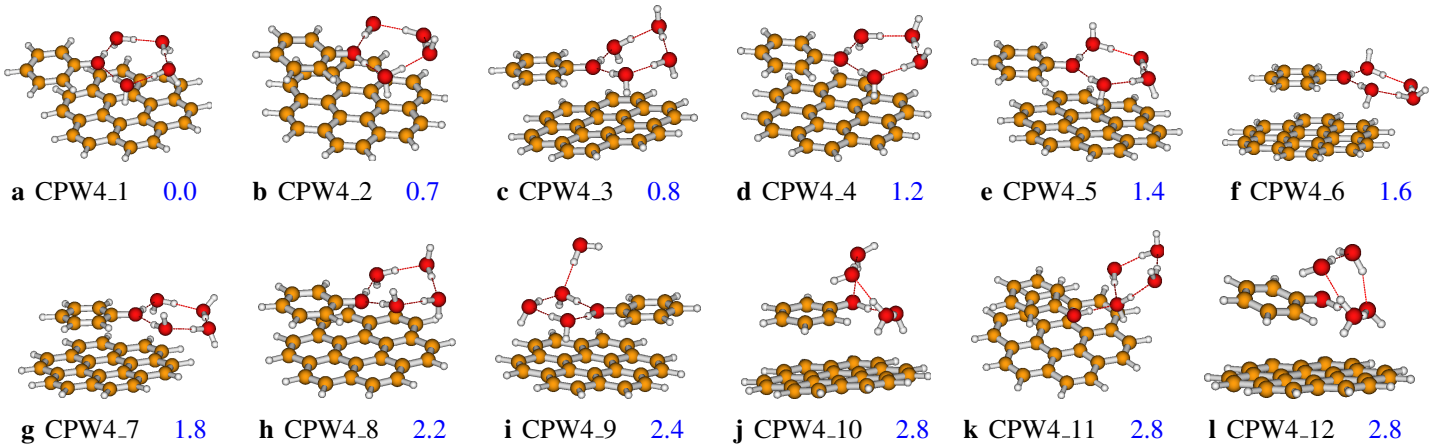

Fig. 5 Twelve most stable structures of Coronene-PhOH$(H_2O)_4$ as optimised at the ωB97XD/aug-cc-pVDZ level of theory. The structures are optimised in implicit water solvent using the PCM solvation model. Numbers represent the relative electronic energies of the structures (in kcal/mol), and calculated at the ωB97XD/aug-cc-pVDZ level of theory. The complete list of the optimised structures is provided in the supporting information.

ergy at room temperature (-1.3 kcal/mol) could be due to the failure of the proposed model. In fact, the small value of the adsorption free energy indicates that coronene is not a suitable material for the adsorption of phenol. This is perfectly understandable, as the only possible interaction between phenol and coronene comes from weak $\pi\cdots\pi$ bonding interactions. Adsorption of phenol onto a surface that can establish strong covalent or non-covalent bonding with phenol would yield a more negative value of the adsorption free energy. The adsorption of phenol onto pristine graphene has been reported by Liu *et al.*[7]. They calculated the adsorption electronic energy to be -20.3 kcal/mol. When one pristine carbon atom is doped by a nitrogen atom, the adsorption electronic energy is found to be -21.3 kcal/mol. This result clearly indicates the enhancement of the adsorption energy when the surface can establish strong bondings with the pollutant. Recently, Zhou *et al.*[5] have compared the adsorption of acetone onto an activated carbon (graphene) and some metal oxide surfaces. The authors found that the adsorption electronic energy using the activated carbon is evaluated to be -2.8 kcal/mol. However, when the metal oxide surfaces are used, the adsorption electronic energy is evaluated to be -8.2 kcal/mol (MgO), -14.7 kcal/mol (ZnO) and -4.4 kcal/mol (CuO).

4 Conclusions

In this work, we assessed the effects of solvation and temperature on the adsorption of phenol onto coronene. Although, phenol and coronene are used in this study, the methods used in this work are general and could be applied to any pollutant and any adsorbent. To undertake the investigation, we proposed a methodological approach to compute the adsorption free energy for temperature

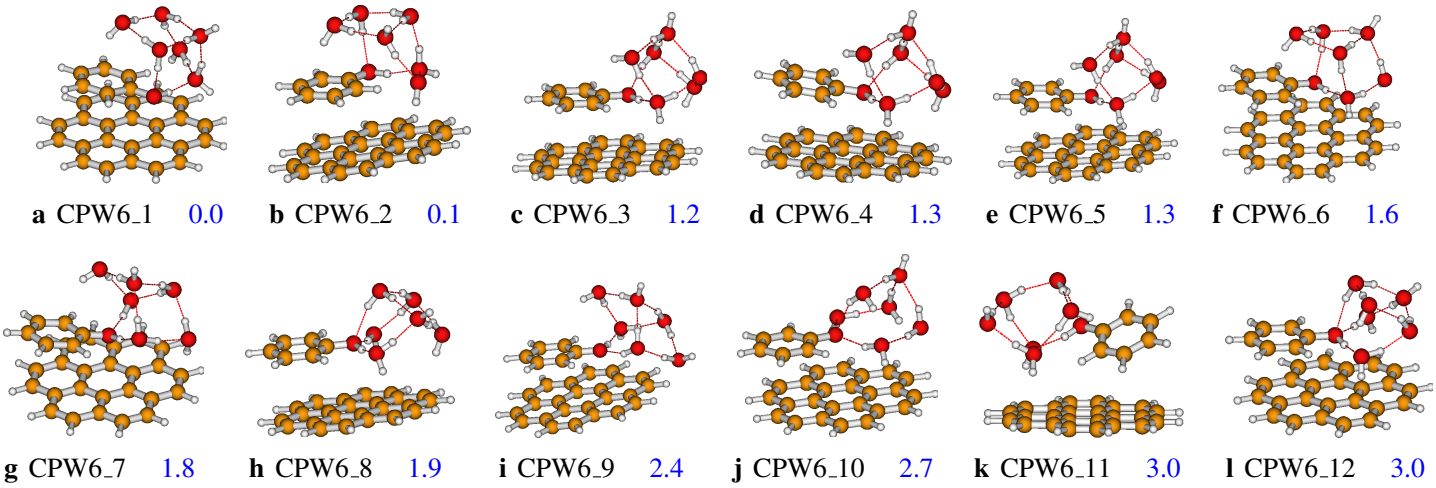

Fig. 6 Twelve most stable structures of Coronene-PhOH$(H_2O)_6$ as optimised at the ωB97XD/aug-cc-pVDZ level of theory. The structures are optimised in implicit water solvent using the PCM solvation model. Numbers represent the relative electronic energies of the structures (in kcal/mol), and calculated at the ωB97XD/aug-cc-pVDZ level of theory. The complete list of the optimised structures is provided in the supporting information.

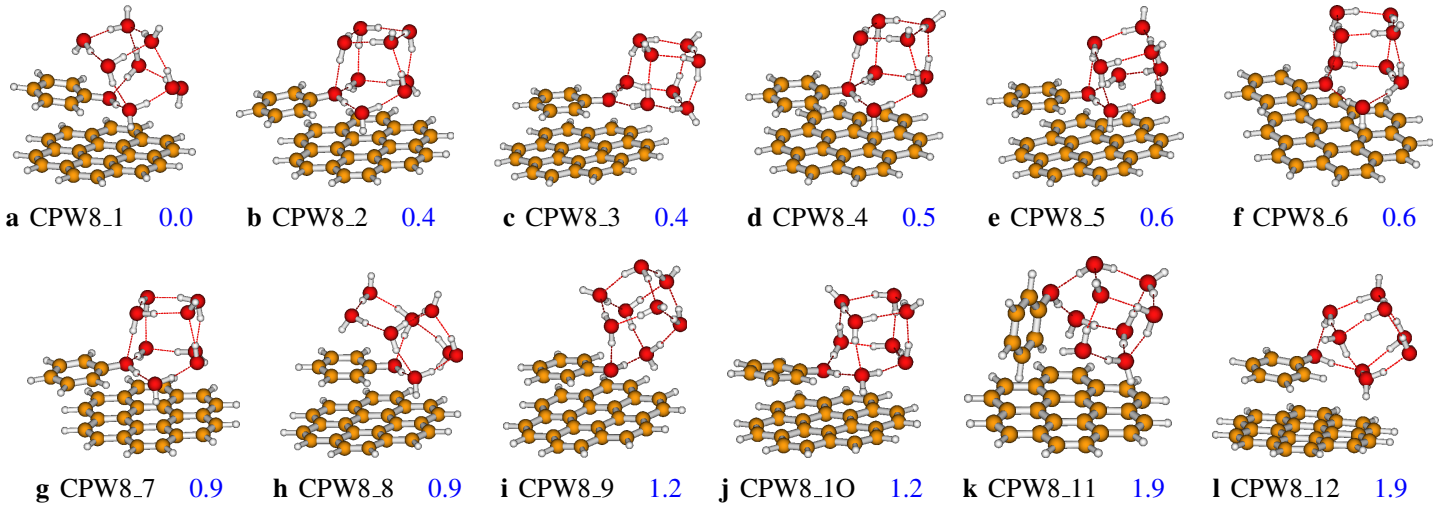

Fig. 7 Twelve most stable structures of Coronene-PhOH$(H_2O)_8$ as optimised at the ωB97XD/aug-cc-pVDZ level of theory. The structures are optimised in implicit water solvent using the PCM solvation model. Numbers represent the relative electronic energies of the structures (in kcal/mol), and calculated at the ωB97XD/aug-cc-pVDZ level of theory. The complete list of the optimised structures is provided in the supporting information.

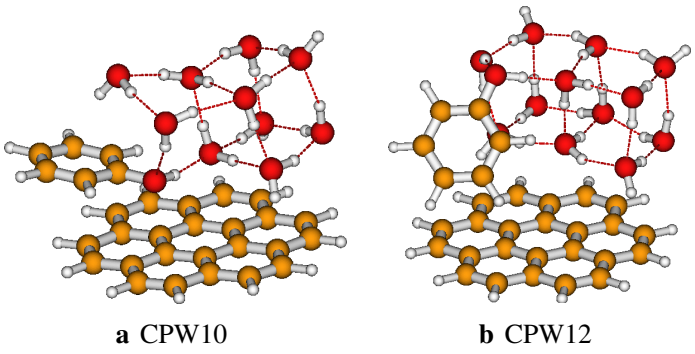

Fig. 8 Most stable structures of Coronene-PhOH$(H_2O)_n$, $n = 10$, and $n = 12$, as optimised at the ωB97XD/aug-cc-pVDZ level of theory. The structures are optimised in implicit water solvent using the PCM solvation model.

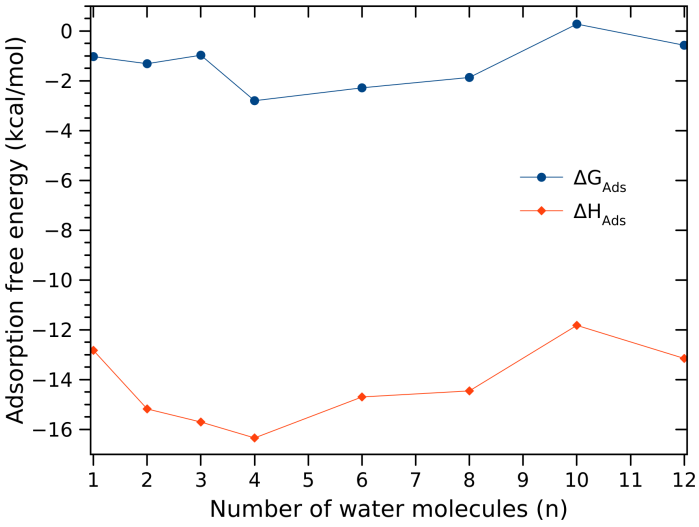

Fig. 9 Calculated adsorption free energy and enthalpy as function of the number of explicit water molecule n at room temperature.

ranging from 200 to 400 K. The solvent effects are considered through hybrid solvation model, where explicit water molecules around the system are treated quantum mechanically, and the remaining water molecules are considered as a dielectric medium, and treated using the PCM solvation model. We considered $n = 1$ to $n = 12$ explicit water molecules. The initial configurations are generated using ABCluster, implementing classical molecular dynamics simulations. The generated configurations are optimised at the ωB97XD/aug-cc-pVDZ level of theory. One configuration comprises one coronene molecule, one phenol molecule and n water molecules.

We have first presented the structures of Coronene-PhOH$(H_2O)_n$ (CPW$_n$) before discussing the adsorption free energy. The results show that the structures of CPW$_n$ are stabilised by strong OH$\cdots$O hydrogen bondings, weak CH$\cdots$O hydrogen bondings, OH$\cdots\pi$ bonding interactions, and $\pi\cdots\pi$ stacking interactions. It has been found that the higher the overlap between the phenyl group and coronene, the higher the stability of the corresponding isomer. In addition, we noted that the configurations formed by the water molecules is similar those of neutral water clusters, and follow the same stability trend.

At room temperature, the adsorption free energy and the adsorption enthalpy are evaluated to be -1.3 kcal/mol and -14.3 kcal/mol, respectively. The results show that the number of explicit water molecules required in the model depends on the hydrophilic region of the system. For the current system (coronene + phenol), one to two explicit water molecules are enough to estimate the adsorption free energy. In addition, it has been found that the adsorption enthalpy is not varying with increasing temperature. The adsorption free energy linearly increases with the increase of temperature.

This work is an attempt to address the effects of solvent and temperature in the molecular modeling of adsorption. Despite the conclusions drawn in this work, there are some limitations that still need to be addressed in future works to maximally approach experimental conditions.

Choice of DFT functional. Although the functional ωB97XD has been extensively benchmarked in previous studies including ours, the functional has been chosen without confirmation of its reliability towards the studied system. For accuracy, one should perform a benchmark study of several DFT functionals to identify the most suitable one.

Implicit solvation. We have used the PCM solvation model. For accuracy, SMD and COSMO solvation models should be also assessed.

Modeling the material. Most of the cheap materials used in experimental studies for adsorption in wastewater treatment are carbon-based materials. These materials are represented usually by activated carbons. In this work, coronene is used to represent the material. In order to approach the experimental conditions, one should populate the surface of coronene or a pristine molecule with active functional groups identified experimentally.

Periodic boundary conditions. For accurate modeling of the process, periodic boundary conditions should be considered for the simulations.

Different pollutants. It would be more reliable to test different pollutants, in the same study, to compare their predicted adsorption free energies and their reported experimental adsorption capacities. This study will serve as a benchmark to the entire modeling of the adsorption process.

Acknowledgements

A.M. is grateful to Prof Lyudmila Moskaleva (Department of Chemistry, University of the Free State) for fruitful discussions. The authors are grateful to the Center for High Performance Computing (CHPC) in South Africa for granting them access to their clusters and computational resources. The Norwegian Supercomputing Program (UNINETT Sigma2, Grant No. NN9684K) is acknowledged for computer time. We would also like to thank the Central Research Fund of the University of the Free State.

Disclosure statement

There are no conflicts of interest to declare.

Data availability statement

The data used in this work is provided in the manuscript or in the supporting information.

Supporting information

Complete lists of the optimised structures of Coronene-$PhOH(H_2O)_n$, $n = 4-8$, and their relative electronic energies are provided herein. In addition, Cartesian coordinates of the optimised geometries are provided. The data used to plot Figure 9 and Figure 10 are also provided.

References

1 Cam, L. M.; Van Khu, L.; Ha, N. N. Theoretical study on the adsorption of phenol on activated carbon using density functional theory. *J. Mol. Model.* **2013**, *19*, 4395–4402.

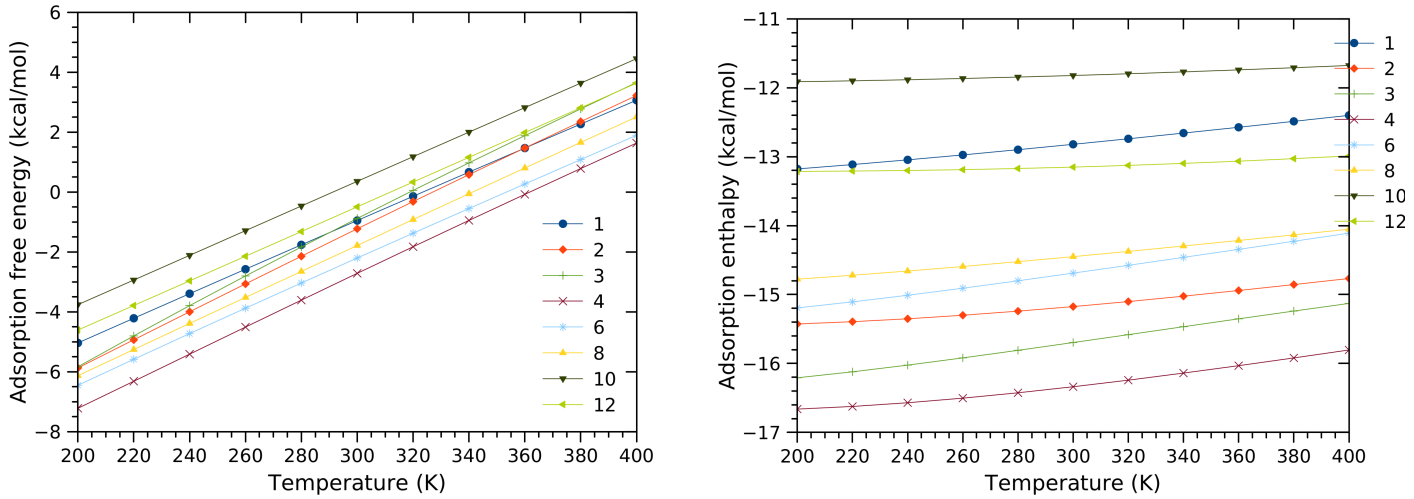

(a) Adsorption free energy (b) Adsorption enthalpy

Fig. 10 Adsorption free energy and adsorption enthalpy for temperatures ranging from 200 to 400 K. The adsorption free energy and enthalpy are calculated for each number n of explicit water molecules.

2 Húmpola, P.; Odetti, H. S.; Albesa, A. G.; Vicente, J. L. Adsorption of phenols from different solvents on graphene: semi-empirical quantum mechanical calculations. *Adsorp. Sci. Technol.* **2013**, *31*, 359–371.

3 Li, H.; Liu, Y.; Yang, Y.; Yang, D.; Sun, J. Influences of hydrogen bonding dynamics on adsorption of ethyl mercaptan onto functionalized activated carbons: a DFT/TDDFT study. *J. Photochem. Photobiol. A* **2014**, *291*, 9–15.

4 Bahamon, D.; Carro, L.; Guri, S.; Vega, L. F. Computational study of ibuprofen removal from water by adsorption in realistic activated carbons. *J. Colloid Interface Sci.* **2017**, *498*, 323–334.

5 Zhou, K.; Ma, W.; Zeng, Z.; Ma, X.; Xu, X.; Guo, Y.; Li, H.; Li, L. Experimental and DFT study on the adsorption of VOCs on activated carbon/metal oxides composites. *J. Chem. Eng.* **2019**, *372*, 1122–1133.

6 Li, S.; Song, K.; Zhao, D.; Rugarabamu, J. R.; Diao, R.; Gu, Y. Molecular simulation of benzene adsorption on different activated carbon under different temperatures. *Microporous Mesoporous Mater.* **2020**, *302*, 110220.

7 Liu, X.; Han, Y.; Cheng, Y.; Xu, G. Microwave-assisted ammonia modification of activated carbon for effective removal of phenol from wastewater: DFT and experiment study. *Appl. Surf. Sci.* **2020**, *518*, 146258.

8 Malloum, A.; Conradie, J. Molecular simulations of the adsorption of aniline from waste-water. *J. Mol. Graph. Mod.* **2022**, *117*, 108287.

9 Fifen, J. J.; Nsangou, M.; Dhaouadi, Z.; Motapon, O.; Jaidane, N.-E. Structures of Protonated Methanol Clusters and Temperature Effects. *J. Chem. Phys.* **2013**, *138*, 184301.

10 Fifen, J. J.; Agmon, N. Structure and spectroscopy of hydrated sodium ions at different temperatures and the cluster stability rules. *J. Chem. Theory Comput.* **2016**, *12*, 1656–1673.

11 Zhang, J.; Dolg, M. ABCluster: the artificial bee colony algorithm for cluster global optimization. *Phys. Chem. Chem. Phys.* **2015**, *17*, 24173–24181.

12 Zhang, J.; Dolg, M. Global optimization of clusters of rigid molecules using the artificial bee colony algorithm. *Phys. Chem. Chem. Phys.* **2016**, *18*, 3003–3010.

13 Vanommeslaeghe, K.; Hatcher, E.; Acharya, C.; Kundu, S.; Zhong, S.; Shim, J.; Darian, E.; Guvench, O.; Lopes, P.; Vorobyov, I., et al. CHARMM general force field: A force field for drug-like molecules compatible with the CHARMM all-atom additive biological force fields. *J. Comput. Chem.* **2010**, *31*, 671–690.

14 Malloum, A.; Fifen, J. J.; Conradie, J. Large-Sized Ammonia Clusters and Solvation Energies of the Proton in Ammonia. *J. Comput. Chem.* **2020**, *41*, 21–30.

15 Malloum, A.; Fifen, J. J.; Conradie, J. Theoretical infrared spectrum of the ethanol hexamer. *Int. J. Quantum Chem.* **2020**, *120*, e26234.

16 Malloum, A.; Conradie, J. Global and local minima of protonated acetonitrile clusters. *New J. Chem.* **2020**, *44*, 17558–17569.

17 Malloum, A.; Conradie, J. Solvent Effects on the Structures of the Neutral Ammonia Clusters. *Comput. Theor. Chem.* **2020**, *1191*, 113042.

18 Malloum, A.; Conradie, J. Structures of water clusters in the solvent phase and relative stability compared to gas phase. *Polyhedron* **2021**, *193*, 114856.

19 Frisch, M. J. et al. Gaussian˜16 Revision A.03. 2016; Gaussian Inc. Wallingford CT.

20 Chai, J.-D.; Head-Gordon, M. Long-range corrected hybrid density functionals with damped atom–atom dispersion corrections. *Phys. Chem. Chem. Phys.* **2008**, *10*, 6615–6620.

21 Kendall, R. A.; Dunning Jr, T. H.; Harrison, R. J. Electron affinities of the first-row atoms revisited. Systematic basis sets and wave functions. *J. Chem. Phys.* **1992**, *96*, 6796–6806.

22 Malloum, A.; Fifen, J. J.; Conradie, J. Binding energies and isomer distribution of neutral acetonitrile clusters. *Int. J. Quantum Chem.* **2020**, *120*, e26221.

23 Malloum, A.; Fifen, J. J.; Conradie, J. Exploration of the Potential Energy Surfaces of Small Ethanol Clusters. *Phys. Chem. Chem. Phys.* **2020**, *22*, 13201–13213.

24 Malloum, A.; Conradie, J. Accurate binding energies of ammonia clusters and benchmarking of hybrid DFT functionals. *Comput. Theor. Chem.* **2021**, *1200*, 113236.

25 Malloum, A.; Conradie, J. Non-Covalent Interactions in Dimethylsulfoxide (DMSO) Clusters and DFT Benchmarking. *J. Mol. Liq.* **2022**, *350*, 118522.

26 Pinski, P.; Riplinger, C.; Valeev, E. F.; Neese, F. Sparse maps – A systematic infrastructure for reduced-scaling electronic structure methods. I. An efficient and simple linear scaling local MP2 method that uses an intermediate basis of pair natural orbitals. *J. Chem. Phys.* **2015**, *143*, 034108.

27 Riplinger, C.; Pinski, P.; Becker, U.; Valeev, E. F.; Neese, F. Sparse maps – A systematic infrastructure for reduced-scaling electronic structure methods. II. Linear scaling domain based pair natural orbital coupled cluster theory. *J. Chem. Phys.* **2016**, *144*, 024109.

28 Watanabe, H.; Iwata, S. Theoretical studies of geometric structures of phenol-water clusters and their infrared absorption spectra in the O–H stretching region. *J. Chem. Phys.* **1996**, *105*, 420–431.

29 Roth, W.; Schmitt, M.; Jacoby, C.; Spangenberg, D.; Janzen, C.; Kleinermanns, K. Double resonance spectroscopy of phenol$(H_2O)_{1-12}$: Evidence for ice-like structures in aromate–water clusters? *Chem. Phys.* **1998**, *239*, 1–9.

30 Janzen, C.; Spangenberg, D.; Roth, W.; Kleinermanns, K. Structure and vibrations of phenol$(H_2O)_{7,8}$ studied by infrared-ultraviolet and ultraviolet-ultraviolet double-resonance spectroscopy and ab initio theory. *J. Chem. Phys.* **1999**, *110*, 9898–9907.

31 Guedes, R.; Costa Cabral, B.; Martinho Simoes, J.; Diogo, H. Thermochemical Properties and Structure of Phenol-$(H_2O)_{1-6}$ and Phenoxy-$(H_2O)_{1-4}$ by Density Functional Theory. *J. Phys. Chem. A* **2000**, *104*, 6062–6068.

32 Ahn, D.-S.; Jeon, I.-S.; Jang, S.-H.; Park, S.-W.; Lee, S.-Y.; Cheong, W.-J. Hydrogen bonding in aromatic alcohol-water clusters: A brief review. *Bull. Korean Chem. Soc.* **2003**, *24*, 695–702.

33 Parthasarathi, R.; Subramanian, V.; Sathyamurthy, N. Hydrogen bonding in phenol, water, and phenol- water clusters. *J. Phys. Chem. A* **2005**, *109*, 843–850.

34 Shields, R. M.; Temelso, B.; Archer, K. A.; Morrell, T. E.; Shields, G. C. Accurate predictions of water cluster formation,$(H_2O)_{n=2-10}$. *J. Phys. Chem. A* **2010**, *114*, 11725–11737.

35 Temelso, B.; Archer, K. A.; Shields, G. C. Benchmark Structures and Binding Energies of Small Water Clusters with Anharmonicity Corrections. *J. Phys. Chem. A* **2011**, *115*, 12034–12046.

36 Malloum, A.; Fifen, J. J.; Dhaouadi, Z.; Engo, S. G. N.; Conradie, J. Structures, Relative Stabilities and Binding Energies of Neutral Water Clusters,$(H_2O)_{2-30}$. *New J. Chem.* **2019**, *43*, 13020–13037.

37 Liu, X.; Lu, W.-C.; Wang, C.; Ho, K. Energetic and fragmentation stability of water clusters $(H_2O)_n$, n = 2-30. *Chem. Phys. Lett.* **2011**, *508*, 270–275.

38 Miliordos, E.; Aprà, E.; Xantheas, S. S. Optimal geometries and harmonic vibrational frequencies of the global minima of water clusters $(H_2O)_n$, $n = 2-6$, and several hexamer local minima at the CCSD(T) level of theory. *J. Chem. Phys.* **2013**, *139*, 114302.

39 Pérez, C.; Zaleski, D. P.; Seifert, N. A.; Temelso, B.; Shields, G. C.; Kisiel, Z.; Pate, B. H. Hydrogen Bond Cooperativity and the Three-Dimensional Structures of Water Nonamers and Decamers. *Angew. Chem. Int. Ed.* **2014**, *53*, 14368–14372.

40 Miliordos, E.; Xantheas, S. S. An accurate and efficient computational protocol for obtaining the complete basis set limits of the binding energies of water clusters at the MP2 and CCSD(T) levels of theory: Application to $(H_2O)_m$, $m = 2-6$, 8, 11, 16, and 17. *J. Chem. Phys.* **2015**, *142*, 234303.

41 Bakó, I.; Mayer, I. Hierarchy of the collective effects in water clusters. *J. Phys. Chem. A* **2016**, *120*, 631–638.

42 Tsai, C.; Jordan, K. Monte Carlo simulation of $(H_2O)_8$: Evidence for a low-energy S_4 structure and characterization of the solid$\longleftrightarrow$ liquid transition. *J. Chem. Phys.* **1991**, *95*, 3850–3853.

43 Tsai, C.; Jordan, K. Theoretical study of the $(H_2O)_6$ cluster. *Chem. Phys. Lett.* **1993**, *213*, 181–188.

44 Tsai, C.; Jordan, K. Theoretical study of small water clusters: low-energy fused cubic structures for $(H_2O)_n$, n= 8, 12, 16, and 20. *J. Phys. Chem.* **1993**, *97*, 5208–5210.

45 Song, Y.; Chen, H.; Zhang, C.; Zhang, Y.; Yin, Y. Characteristics of hydrogen bond revealed from water clusters. *Eur. Phys. J. D* **2014**, *68*, 242.

46 Yang, L.; Ji, H.; Liu, X.; Lu, W.-C. Ring-Stacking Water Clusters: Morphology and Stabilities. *ChemistryOpen* **2019**, *8*, 210–218.

47 Zhang, B. et al. Infrared spectroscopy of neutral water clusters at finite temperature: Evidence for a noncyclic pentamer. *Proc. Natl. Acad. Sci.* **2020**, *117*, 15423–15428.

48 Rakshit, A.; Bandyopadhyay, P.; Heindel, J. P.; Xantheas, S. S. Atlas of putative minima and low-lying energy networks of water clusters $n = 3-25$. *J. Chem. Phys.* **2019**, *151*, 214307.